# Nonlinear optical susceptibility of deformed achiral carbon nanotubes studied from first-principles calculations

Jian Zhou, Hongming Weng, Gang Wu, and Jinming Dong[a)]
*Group of Computational Condensed Matter Physics, Department of Physics and National Laboratory of Solid State Microstructures, Nanjing University, Nanjing 210093, People's Republic of China*

(Received 3 January 2006; accepted 29 May 2006; published online 5 July 2006)

The second harmonic generation (SHG) coefficients of the deformed single-walled carbon nanotubes (SWNTs) have been calculated from the density functional theory in the local density approximation. The obtained results show that their nonlinear responses are very sensitive to the deformation degree and the helicity of the SWNTs, as well as the type of applied strains. More importantly and interestingly, the SHG can be induced in the armchair or zigzag nanotubes under torsional strain, making them promising nonlinear optical materials controllable by applied strains. © *2006 American Institute of Physics*. [DOI: 10.1063/1.2218814]

Carbon nanotubes (CNTs) are hollow cylinders rolled up from graphite sheets with their diameters ranging from several to a few tens of angstroms and their lengths from several micrometers to millimeters. Since their discovery in 1991,[1] a great progress in the researches of their fundamental properties and potential applications has been made in the last decade. Because of their one-dimensional character, CNTs have shown many unusual physical properties and great potential applications in nanotechnology. For example, the CNT can be metallic or semiconducting, depending only on its diameter and the chirality.

In experiments, the CNTs are usually deposited on a substrate, so their deformation is unavoidable, which will introduce some modifications on their electronic structures and further their physical properties.[2,3] It has been found that in the deformed single-walled carbon nanotubes (SWNTs) under uniaxial and torsional strains, their $\pi$ orbital electronic band structures are determined by their chiral symmetries and strains.[4–6] Most of the deformed SWNTs show a metal-semiconductor transition, occurring repeatedly with increase of the strains. Under a uniaxial strain, the energy gap of a zigzag tube varies linearly with the strain and is independent of its diameter, while the armchair tube remains metallic. In contrast, under a torsional strain, the energy gap changes most for the armchair tubes, while the metallic zigzag tube remains metallic. All the changes of electronic structures of the SWNTs would influence their optical properties sensitively. Then, the studies on the linear and nonlinear optical properties of the deformed SWNTs could be helpful in determining accurately the geometrical structures of SWNTs in experiment.

In fact, many theoretical studies on the optical properties of the SWNTs have been done mainly based on the tight-binding approximation.[7–13] For example, Jiang *et al.* have studied the linear optical properties of the deformed SWNTs using an analytical $\pi$-band tight-binding calculation.[10] However, there are only a few of the more accurate *ab initio* studies on these so far,[14–17] which could be more applicable to the SWNTs with smaller diameters and deformed SWNTs. Recently, a systematic *ab initio* study on the optical properties of the SWNTs has been done by Guo *et al.*[18] They calculated the optical dielectric function and second-order optical susceptibility for a lot of armchair, zigzag, and chiral SWNTs, and found that the energy position, the shape, and the number of absorption peaks of small diameter nanotubes depend rather strongly on their diameters and chiralities. It is also revealed that the magnitude of the second-order optical susceptibility of small chiral SWNTs is very large, even reaching nearly ten times larger than that of GaAs, suggesting that the small chiral SWNTs could be a good nonlinear optical material.[18]

It is well known that the inversion symmetry eliminates the second harmonic generation (SHG), making the achiral SWNTs, i.e., the armchair and zigzag ones, have no SHG. However, an application of a torsional strain can break the inversion symmetry of achiral SWNTs and will hopefully induce SHG signals in them. So, in this letter, we will try to make the first-principles calculations for studying the deformation effects on the optical responses in SWNTs and pay more attention to the deformation-induced SHG in the SWNTs.

We use the total energy plane-wave pseudopotential method in the local density approximation (LDA) with the Ceperley-Alder exchange correlation. The Vienna *ab initio* simulation package[19,20] (VASP) is employed. The interaction between the ions and electrons is described by the highly accurate full-potential projected augmented wave (PAW),[21,22] which can give a more accurate and reliable result than the ultrasoft potential. In our calculations, the $2s$ and $2p$ orbitals of the carbon atom are treated as valence orbitals, and a large plane-wave cutoff of 450 eV is used throughout.

A supercell geometry is adopted so that the nanotubes are aligned in a hexagonal array, with the closest distance between adjacent nanotubes being at least 10 Å. The tube axial is along the $z$ direction, and a uniform grid of $1\times1\times n$ $k$ points is used, and the maximum spacing between $k$ points is less than 0.01 $Å^{-1}$. The special $k$ point method plus the Gaussian broadening technique (with a Gaussian width of 0.05 eV) are used in the Brillouin zone integration.

We first construct an ideal nanotube from a graphite sheet. Then, a conjugate gradient method is used to optimize the positions of atoms and also the supercell height, until the

[a)]Author to whom correspondence should be addressed; electronic mail: jdong@nju.edu.cn

 

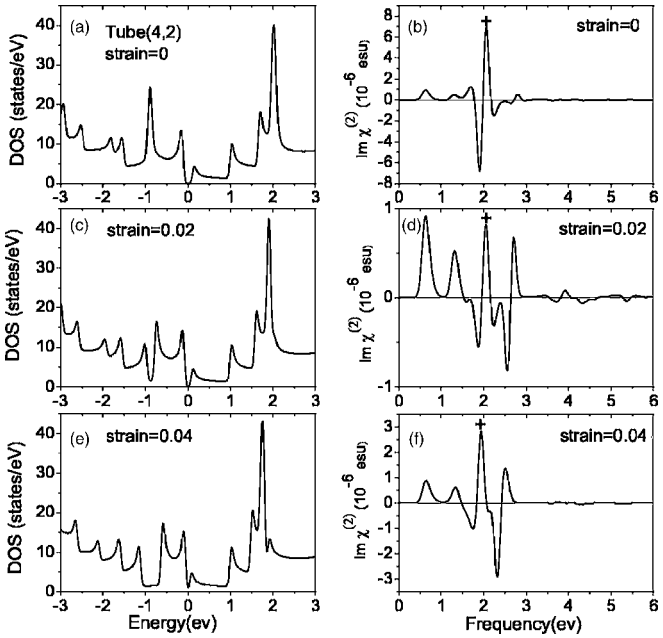


FIG. 1. Density of states (left three panels, $E_f$=0) and Im $\chi^{(2)}_{xyz}$ (right three panels) of the (4, 2) chiral SWNT under different tensile strains.

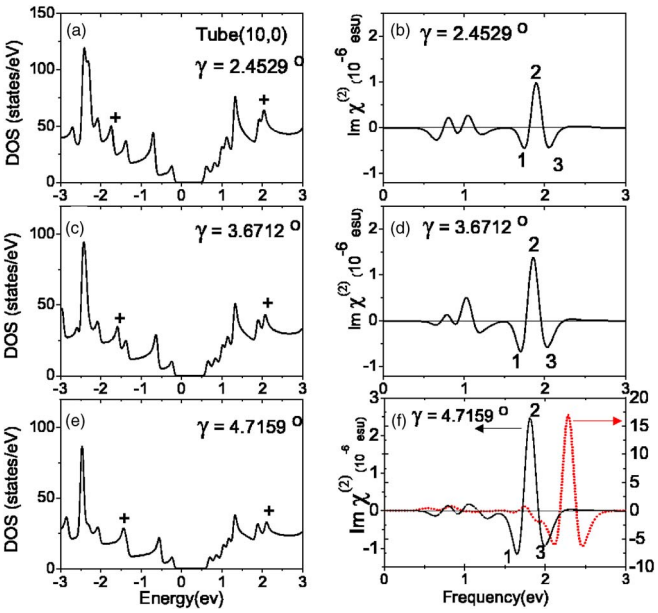


FIG. 2. (Color online) Density of states (left three panels, $E_f$=0) and Im $\chi^{(2)}_{xyz}$ (right three panels) of the (10,0) SWNT under different torsional strains. In Fig. 2(f), the red dotted line is the calculated SHG for the SWNT (10, 0) bundle under 4.7159° torsional strain. The main peaks are listed in Table I.

forces acting on all the atoms are less than 0.01 eV/Å. With the equilibrium structure, we then use a more dense set of $k$ points to calculate the electronic structure and the momentum matrix elements.[23] And finally we use the same formulas as in Ref. 18 to obtain the dielectric function and the SHG susceptibility. The formulas are obtained in the independent particle approximation,[24,25] and used also to calculate the dielectric function of graphite, showing a good agreement with experiments.[18]

The SHG of several deformed SWNTs are firstly calculated. Here, we only present in Fig. 1 the density of states (DOS) and the imaginary part (Im $\chi^{(2)}_{xyz}$) of the SHG for the chiral (4,2) tube under tensile strain. It is seen that the undeformed (4,2) tube is a semiconductor with a small gap of about 0.1 eV, and its highest SHG peak is located at about 2 eV with its absolute value of about $10\times10^{-6}$ esu, which is consistent with the previous result.[18]

The tensile strain shifts the DOS peaks obviously, making the DOS gap disappear at 4% tensile strain. And it also changes the SHG. However, the curve shape and the peaks of its SHG under different tensile strains are quite similar, except for the peak shift and the change of peak height under the strain. For example, the peaks labeled + in Figs. 1(b), 1(d), and 1(f), are located at 2.07, 2.05, and 1.94 eV under the 0, 0.02, and 0.04 tensile strains, respectively.

We then pay more attention to the SHG of deformed achiral SWNTs under torsional strain because both the perfect armchair and zigzag nanotubes do not have SHG due to their inversion symmetries, and the uniaxial strain does not break their inversion symmetries. The calculated results for a (10,0) zigzag SWNT and a (5,5) armchair SWNT are shown in Figs. 2 and 3, respectively, from which it is clearly seen that the SHG signal can indeed be observed, and its amplitude is very large too.

The SHG peaks can also be explained by the corresponding DOSs. Since the SHG is a two photon excitation process, it is more complex than the linear optical response. For example, the two DOS peaks, labeled by the symbol + in Fig. 2(a) and located at −1.74 and 2.04 eV, produce the highest SHG peak 2 in Fig. 2(b), located at 1.89 eV.

The SHG peaks can be shifted by the torsional strains, which can be explained by the shift of the DOS peaks. For example, for the (10, 0) zigzag tube when its torsional deformation is increased to 3.6712° as shown in Fig. 2(c), the two DOS + peaks shift to −1.60 and 2.07 eV, making the corresponding SHG peak 2 in Fig. 2(d) shift to 1.86 eV. Again, in Fig. 2(e), the two DOS + peaks shift to −1.44 and 2.10 eV due to more increased torsional strain, and so the corresponding SHG peak 2 in Fig. 2(f) shifts further to 1.81 eV.

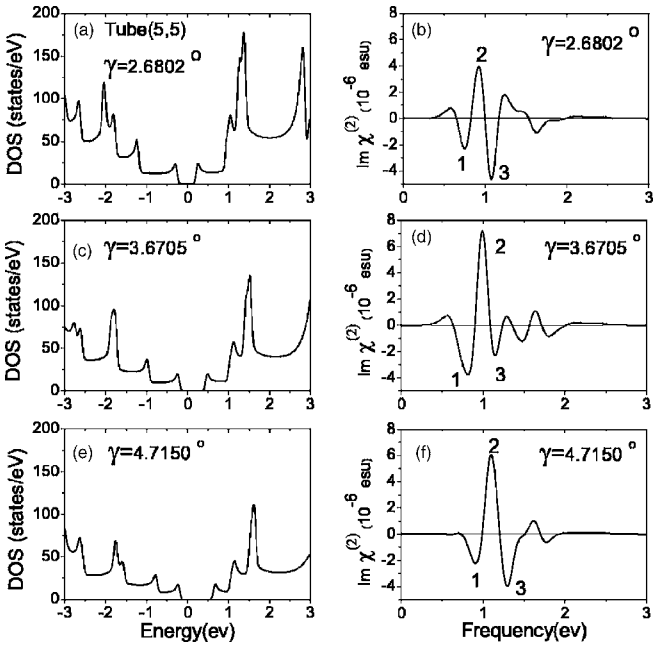


FIG. 3. Density of states (left three panels, $E_f$=0) and Im $\chi^{(2)}_{xyz}$ (right three panels) of the (5, 5) SWNT under different torsional strains. The main peaks are listed in Table II.

TABLE I. Calculated positions of three Im $\chi^{(2)}_{xyz}(-2\omega;\omega,\omega)$ peaks of the (10,0) SWNT under torsional deformation. The peak labels are marked in Fig. 2. The values in the brackets are frequency shifts relative to those under previous torsional strain. The frequency unit is eV.

| Torsional | 2.4529° | 3.6712° | 4.7159° |
|---|---|---|---|
| Peak 1 | 1.74 | 1.70 (−0.04) | 1.65 (−0.05) |
| Peak 2 | 1.89 | 1.86 (−0.03) | 1.81 (−0.05) |
| Peak 3 | 2.05 | 2.03 (−0.02) | 2.00 (−0.03) |

TABLE II. The same as Table I except for the (5,5) SWNT. The peak labels are marked in Fig. 3.

| Torsional | 2.6802° | 3.6705° | 4.7150° |
|---|---|---|---|
| Peak 1 | 0.75 | 0.82 (0.07) | 0.91 (0.09) |
| Peak 2 | 0.92 | 0.99 (0.07) | 1.10 (0.11) |
| Peak 3 | 1.07 | 1.14 (0.07) | 1.29 (0.15) |

Finally, we should emphasize that in our calculations, in order to obtain a reasonable SHG amplitude of an isolated SWNT, we have used the effective unit cell volume of the SWNTs, rather than their supercell volume.[18] For identifying its reliability, we have also calculated the SHG of a SWNT (10,0) bundle under 4.7159° torsional strain because the tube bundle is a realistic bulk material and has a well defined unit cell volume. The obtained SHG result of the bundle is presented in Fig. 2(f), from which it is clearly seen that except for the blueshift of the peak position, the peak amplitude of the SWNT bundle's SHG is even larger than that of the isolated SWNT, and also than those of GaAs and GaP.[26] Therefore, the effective unit cell volume we used in above calculations is reliable, and the calculated SHG values for the deformed SWNTs are meaningful, which could be comparable with those of the bulk nonlinear optical materials.

The main peaks in Figs. 2 and 3 are listed in Tables I and II, respectively. By a comparison of these, we find that the main peaks of zigzag (10,0) SWNT shift little under the torsional strain (less than 0.05 eV/deg), while those of the armchair (5,5) SWNT shift more under almost the same torsional strain (about 0.1 eV/deg). This is because the electronic structure of the armchair tube is more sensitive to the torsional strain than the zigzag tube. Also, we can see clearly from Fig. 3 and Table II that the highest SHG peak of SWNT (5,5) shifts towards the higher energy with increasing torsional strain. So, the shifting of the main peaks in the SHG of the deformed SWNTs could reflect the strength of the applied torsional strain on them.

Since it is difficult to observe directly the geometrical structures of the SWNTs, and probably more difficult to know if a SWNT is subject to deformation or not, the effects of the applied strains on the nonlinear optical responses found in this letter could be quite important for experiments, based on which the deformation degree of the SWNTs, the type of applied strains, and the helicity of the SWNTs could be determined accurately in experiments.

In summary, using the first-principles method, we have calculated the nonlinear optical responses of the deformed SWNTs, and more attention has been paid to those of the achiral SWNTs under the torsional strains. Our *ab initio* calculations found that the tensile strain can shift the SHG peaks and change their heights for the chiral SWNTs. More importantly, it is found that the torsional strain can induce the nonlinear SHG optical signals in the deformed achiral SWNTs, which should be exactly zero in the undeformed SWNTs with an inversion symmetry. And the amplitude of the torsional-strain-induced SHG signal is larger enough for experimental measurements, suggesting that it has a potential application in the future nonlinear optical materials with advantage of controlling the creation or annihilation of the SHG signals by switching on or off an applied torsional strain.

This work was supported by the Natural Science Foundation of China under Grant Nos. 10474035 and 90503012, and also from a Grant for State Key Program of China through Grant No. 2004CB619004.

[1] S. Iijima, Nature (London) **354**, 56 (1991).
[2] T. Hertel, R. Martel, and P. Avouris, J. Phys. Chem. B **102**, 910 (1998).
[3] T. Hertel, R. E. Walkup, and P. Avouris, Phys. Rev. B **58**, 13870 (1998).
[4] R. Heyd, A. Charlier, and E. McRae, Phys. Rev. B **55**, 6820 (1997).
[5] L. Yang, M. P. Anantram, J. Han, and J. P. Lu, Phys. Rev. B **60**, 13874 (1999).
[6] L. Yang and J. Han, Phys. Rev. Lett. **85**, 154 (2000).
[7] H. Ajiki and T. Ando, Physica B **201**, 349 (1994).
[8] H. Ajiki, Phys. Rev. B **65**, 233409 (2002).
[9] M. F. Lin, Phys. Rev. B **62**, 13153 (2000).
[10] H. Jiang, G. Wu, X. P. Yang, and J. M. Dong, Phys. Rev. B **70**, 125404 (2004).
[11] V. N. Popov and L. Henrard, Phys. Rev. B **70**, 115407 (2004).
[12] I. Milosević, T. Vuković, S. Dmitrović, and M. Damnjanović, Phys. Rev. B **67**, 165418 (2003).
[13] I. Milosević, B. Nikolić, and M. Damnjanović, Phys. Rev. B **69**, 113408 (2004).
[14] H. J. Liu and C. T. Chan, Phys. Rev. B **66**, 115416 (2002).
[15] M. Machón, S. Reich, C. Thomsen, D. Sánchez-Portal, and P. Ordejón, Phys. Rev. B **66**, 155410 (2002).
[16] C. D. Spataru, S. Ismail-Beigi, L. X. Benedict, and S. G. Louie, Phys. Rev. Lett. **92**, 077402 (2004).
[17] M. F. Ng, S. L. Sun, and R. Q. Zhang, Phys. Rev. B **72**, 033406 (2005).
[18] G. Y. Guo, K. C. Chu, D. S. Wang, and C. G. Duan, Phys. Rev. B **69**, 205416 (2004).
[19] G. Kresse and J. Hafner, Phys. Rev. B **48**, 13115 (1993).
[20] G. Kresse and J. Furthmüller, Comput. Mater. Sci. **6**, 15 (1996).
[21] P. E. Blöchl, Phys. Rev. B **50**, 17953 (1994).
[22] G. Kresse and J. Joubert, Phys. Rev. B **59**, 1758 (1999).
[23] B. Adolph, J. Furthmüller, and F. Bechstedt, Phys. Rev. B **63**, 125108 (2001).
[24] E. Ghahramani, D. J. Moss, and J. E. Sipe, Phys. Rev. B **43**, 8990 (1991).
[25] E. Ghahramani, D. J. Moss, and J. E. Sipe, Phys. Rev. B **43**, 9700 (1991).
[26] J. L. P. Hughes and J. E. Sipe, Phys. Rev. B **53**, 10751 (1996).